A CLOSER LOOK AT THE ABUNDANCE OF MEK IN THE COLORADO FRONT RANGE IN SUMMER 2015

A THESIS

Presented to

The Faculty of the Environmental Program

The Colorado College

In Partial Fulfillment of Requirements for the Degree

Bachelor of Arts

By

Daniel Rodriguez

May/2018

_____
Lynne Gratz
Assistant Professor

_____
Sally Meyer
Professor

TABLE OF CONTENTS

ABSTRACT. The Colorado Northern Front Range Metropolitan Area (NFRMA) regularly exceeds the National Ambient Air Quality Standards (NAAQS) for ozone (O_3). This region has a growing urban population and extensive oil and natural gas production from the nearby Wattenberg Gas Field (WGF) in the Denver-Julesburg Basin. In 2015, a large suite (40+ species) of volatile organic compounds were measured using a custom built online multichannel gas chromatography system over 8 weeks in spring and 8 weeks in summer at the Boulder Atmospheric Observatory (BAO). Abeleira et al. (2017) quantified three oxygenated volatile organic compounds (OVOCs): acetone, acetaldehyde, and methyl ethyl ketone (MEK). Abeleira et al. (2017) found that OVOCs accounted for almost a quarter of the OH reactivity yet the source profiles for these compounds were poorly reconstructed by a Positive Matric Factorization (PMF) analysis. Here, we closely examine the abundance of MEK to better understand the different sources of MEK. MEK can be directly emitted and it can also be produced during the atmospheric oxidation of several different hydrocarbons (e.g. n-butane, 3-methylhexane, i-pentane) however these mechanisms are poorly understood. We investigate the dominant photochemical production pathways using a box model, and characterize local and synoptic meteorological conditions with respect to MEK abundance. We find that emissions of light alkanes (e.g. n-butane) are an important component for understanding mixing ratios of OVOCs, specifically MEK, in the NFRMA.

1. INTRODUCTION

The Colorado Northern Front Range Metropolitan Area (NFRMA) has many sources that contribute to the atmospheric composition of the region. The Denver

Metropolitan Area has high emissions of reactive nitrogen oxides ($NO + NO_2 = NO_x$) while the Wattenberg Gas Field (WGF), in Weld County, has high emissions of hydrocarbons and other volatile organic compounds (VOCs) (Swarthout et al., 2013). These two classes of species, nitrogen oxides (NO_x) and VOCs, are the two necessary reactants for tropospheric ozone (O_3) formation. The WGF (in the Denver-Julesburg Basin) was the fourth largest oil field and ninth largest gas field in the U.S. as of 2013 (EIA, 2015). Additionally, there are semi-rural agricultural emissions of biogenic volatile organic compounds (BVOCs) from the north and east, which can also serve as precursors in the formation of O_3.

The NFRMA regularly exceeded the National Ambient Air Quality Standard (NAAQS) for O_3 over the past decade (Abeleira et al., 2017; Colorado Air Quality Commission, 2008). O_3 production in the lower troposphere occurs when VOCs are oxidized in the presence of NO_x and sunlight. The ability for a VOC to initiate the O_3 production cycle is described by its reactivity with hydroxyl (OH) radicals. In 2008, counties within the Denver Metropolitan Area and Northern Front Range were categorized as nonattainment areas under the Clean Air Act (Colorado Air Quality Commission, 2008). Since 2008, the Colorado state government has implemented programs and regulations in order to curb the emission of NO_x and VOC precursors (Allison, 2015). Furthermore, regulation went into effect in 2008 to curb the emissions from oil and natural gas production facilities. While the state has cut emissions of NO_x and VOCs by approximately 35,000 and 93,000 tons per year, respectively, the region still remained a nonattainment area through 2015 (Allison, 2015).

The NFRMA region experiences higher mixing ratios of C_2-C_6 alkanes relative to other U.S. regions (Abeleira et al., 2017; Baker et al., 2008). Mixing ratios of propane, butane isomers (i- and n-butane), and pentane isomers (i- and n-pentane) exceeded the summer time average mixing ratios in 28 other U.S. cities (Baker et al., 2008). The light alkanes were highly correlated with propane, a known marker for natural gas production during summer 2008 (Petrón et al., 2012). High C_2-C_6 alkane mixing ratios have been observed near the densest drilling operations with lower mixing ratios further from these areas of active oil and natural gas (ONG) extraction and production (Thompson et al., 2014). The WGF employs non-conventional methods of oil and natural gas extraction, such as hydraulic fracturing and horizontal drilling, which can serve as an important emission source of light alkanes and other VOCs (Katzenstein et al., 2003; Colborn et al., 2011). An increase in emissions from these non-conventional methods of ONG extraction were found to have an adverse effect on air quality (McKenzie et al., 2012) and are a concern for human health (Colborn et al. 2011). Previous study found that ONG sources dominate VOC reactivity in the NFRMA (Thompson et al., 2014; Swarthout et al., 2013).

During a sixteen-week, long-term air quality campaign in spring and summer 2015, Abeleira et al. (2017) characterized VOCs in the NFRMA. Abeleira et al. (2017) found that the average VOC reactivity was lower in the NFRMA than in most other US urban areas. Furthermore, an analysis of source profiles using positive matrix factorization (PMF) was used to identify the sources of VOCs in spring and summer. This analysis classified the sources of each component for all the species measured. Abeleira et al. (2017) identified five distinct VOC factors in spring and six VOC factors in

summer. These factors, which are long-lived ONG emissions, short-lived ONG, traffic, background, secondary chemical production, and biogenic (only in summer) showed that VOC emissions in the NFRMA were strongly influenced by anthropogenic emissions of VOCs, specifically emissions from ONG sources. This analysis also showed that traffic-related VOCs were minor contributors to VOC reactivity compared to the substantial contributions by ONG sources. The PMF analysis also showed that the acetone, acetaldehyde, and methyl ethyl ketone were in part associated with background and secondary factors but largely speaking these species were not well-constrained by the PMF solution (<55% of mass and variance). These findings suggested that the secondary sources of these compounds operated on timescales that were quite different from the bulk of the secondary factor or that primary emissions were not captured by the PMF solution (Abeleira et al., 2017). It is also possible that there were source profiles not captured by the PMF solution.

While the PMF analysis could not explain the source profiles behind all mixing ratios, it did show several important factors to the formation and emission of methyl ethyl ketone (MEK). Although Abeleira et al. (2017) found a significant biogenic factor in summer, there was evidence to suggest direct biogenic emissions of MEK did not significantly affect MEK mixing ratios by looking at the relationship between isoprene and MEK ($R = -0.127$, $p = 0.003$). Therefore, mixing ratios of MEK in the NFRMA appeared to be driven by secondary production and direct anthropogenic emission.

The oxygenated volatile organic compounds (OVOCs) account for a large proportion (23%) of the OH reactivity in the NFRMA (Abeleira et al., 2017) yet remained the least constrained of the measured VOCs. Mellouki et al. (2015) found that

degradation of OVOCs in the troposphere lead to the production of a large range of secondary pollutants, such as O_3, highly oxidized VOCs (HOVOCs), peroxyacyl nitrates (PAN), and secondary organic aerosol (SOA). Oxygenated VOCs can also affect the radiative forcing of O_3, which in turn can affect the atmospheric lifetime of known greenhouse gases (Mellouki et al., 2015). Characterizing the OVOCs and their chemistry is important for constraining the OH reactivity and the radical budget of the NFRMA region in order to better understand chemical reactions in the gas-phase (Abeleira et al., 2017). The PMF also showed that OVOCs from direct emissions or secondary production were a major OH radical sink in the NFRMA (Abeleira et al., 2017).

Of these OVOCs, Abeleira et al. (2017) found that MEK had the single largest contribution to the secondary factor (38% of mixing ratios could be attributed to secondary production).

Methyl ethyl ketone (C_4H_8O) is found over a wide range of environments, from pristine rainforest to rural sites to megacities across the world (Yañez-Serrano et al., 2016; Jordan et al., 2009; Liu et al., 2015; Brito et al., 2015). While often measured with other VOCs, MEK has received little attention. While MEK is generally less prevalent in the atmosphere as other OVOCs, such as acetone, MEK is about an order of magnitude more reactive than acetone, with respect to reactions with OH (Atkinson, 2000), making MEK a compound of interest when taking into account the OH budget of a region.

There are several known sources and sinks of MEK but they are not well understood (Jordan et al., 2009; Yañez-Serrano et al., 2016). Biogenic emissions of MEK have been measured from terrestrial vegetation (Muller et al., 2006; Yañez-Serrano et al., 2016; de Gouw et al., 1999; Kirstine et al., 1998), fungi (Wheatley et al., 1997; Gray

et al., 2010), and bacteria (Song and Ryu, 2013). Emissions of MEK constituted 45-50% of VOC emissions from clover pasture in Australia (Kirstine et al., 1998). MEK can also be emitted directly by several anthropogenic sources, including anthropogenic biomass burning (Andreae and Merlet, 2001), solvent evaporation (Kim et al., 2015) and vehicle exhaust (Brito et al., 2015; Liu et al., 2015). While MEK can be emitted from biogenic sources, it is important to note that no mechanistic pathways for MEK have been found for the formation of MEK from isoprene or other dominant biogenic VOCs (Singh et al., 2004).

MEK can also form by atmospheric oxidation of other compounds (Sommariva et al., 2011). The secondary production of MEK results from the photo-oxidation of n-butane and other higher hydrocarbons (de Gouw et al., 2003; Sommariva et al., 2011). This mechanism relies on OH and peroxy radicals (RO_2), which are more prevalent when photochemistry is more active during the day. The MEK yield from n-butane oxidation is on the order of 80% by the following mechanism (Singh et al., 2004):

$$n\text{-}C_2H_5 + OH + (O_2) \rightarrow CH_3C(OO)C_2H_5 + H_2O$$

$$CH_3CH(OO)C_2H_5 + NO \rightarrow CH_3CH(O)C_2H_5 + NO_2$$

$$CH_3CH(O)C_2H_5 + O_2 \rightarrow HO_2 + CH_3C(O)C_2H_5 \quad [\textbf{MEK}]$$

Reaction 1. Mechanism for the formation of MEK from the oxidation of n-Butane.

Furthermore, Sommariva et al. (2011) modeled VOC from the 2002 New England Air Quality study (NEAQS; de Gouw et al, 2005; Goldan et al., 2004) and found that 20-

30% of MEK is formed from the reaction of n-butane with OH. In areas with elevated n-butane mixing ratios, this is expected to be the dominant secondary production mechanism.

There are several known atmospheric sinks of MEK. Removal of OVOCs from the atmosphere occurs by one of three mechanisms: oxidation by OH, photolysis, and/or deposition/surface uptake (Liu et al., 2015). These sinks are not well understood and there is much work to be done on understanding the relative importance of each sink (Singh et al., 2004).

Recent study has also suggested that mixing ratios of MEK could be influenced by long-range transport (Rodigast et al., 2016). MEK has a ~5 day lifetime (against the reaction with OH) and can therefore be transported (Grant et al., 2008; Yañez-Serrano et al., 2016). The oxygenated nature of MEK allows it to interact with water particles in the atmosphere and aqueous surfaces, creating a possible bidirectional exchange of MEK through moist air masses and aqueous surfaces (Sander, 2015; Karl et al., 2005). It is also possible for MEK to be transported by the movement of moist air masses (in rain and cloud water) and, additionally, the liquid-phase fraction of MEK was found to be higher than the expected fraction according to the Henry's Law constant (Grosjean and Wright, 1983; van Pixteren et al., 2005).

This study characterized MEK mixing ratios at the BAO. We examined the photochemical production of MEK, as well as possible mechanisms for non-photochemical production of MEK. For the analysis found in this paper, we focused solely on MEK to explain dominant sources, primarily secondary photochemistry.

2. METHODS

2.1. SITE DESCRIPTION

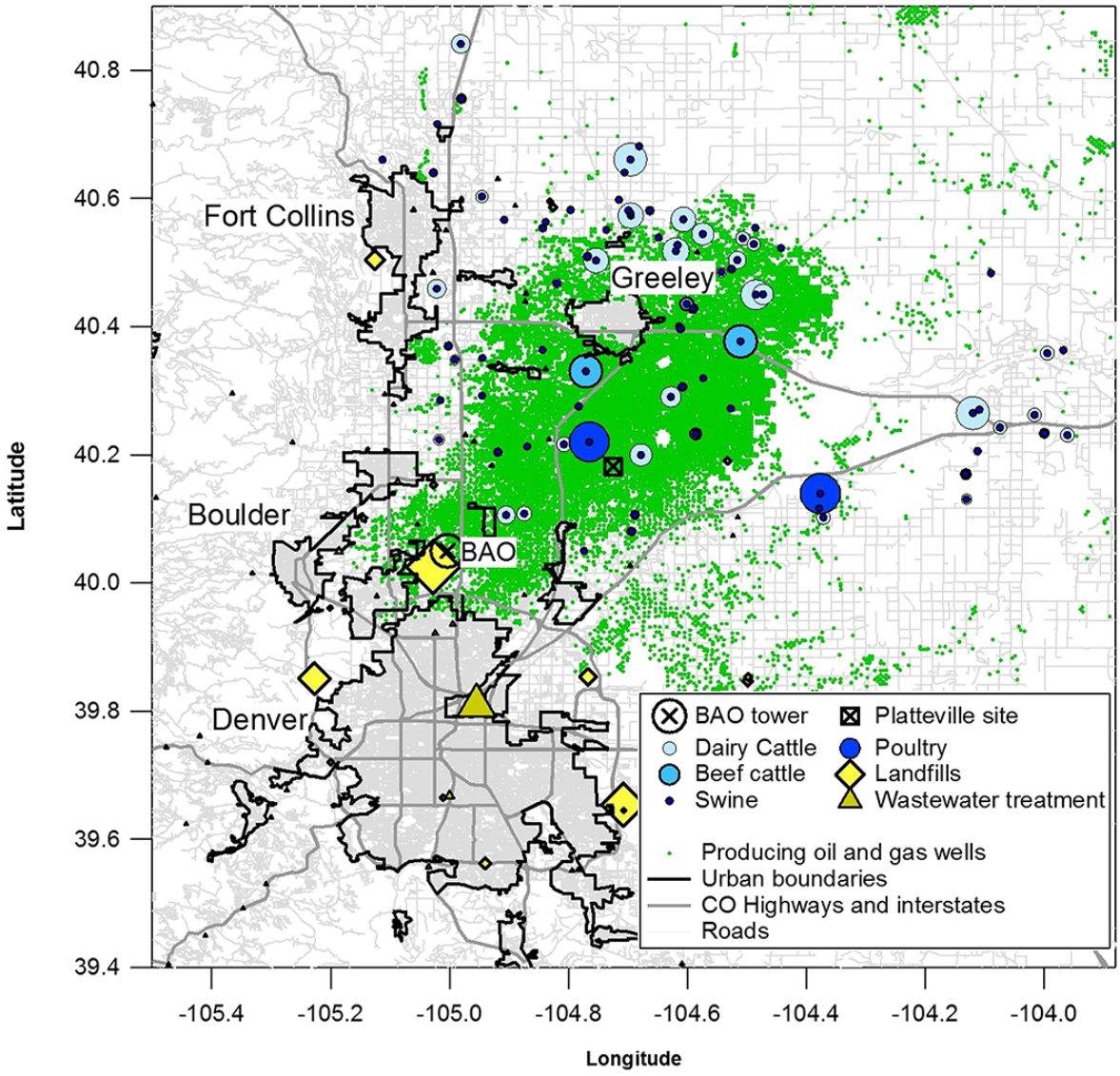

Figure 1. Major urban areas in the Front Range include Fort Collins, Boulder, Denver, and Greeley. The BAO site is at the SW edge of the Wattenberg Gas Field. Active oil and gas wells as of 2012 are represented by green circles (Abeleira et al., 2017). There was significant recent ONG activity near the BAO during the measurement period and likely even more since 2015.

The data was collected at the NOAA Boulder Atmospheric Observatory (BAO) site in Erie, Colorado during two eight-week long periods in the spring (March 20 – May 17) and summer (July 24 – September 6) of 2015. The BAO site is surrounded by primarily agricultural fields. Large urban areas lie to the south (Denver), west (Boulder), north (Fort Collins), and northeast (Greeley). The site is on the southwestern edge of the Wattenberg natural gas field. The BAO site also lies just to the west of I-25, a major transportation corridor along the Front Range (Figure 1).

2.2. MEASUREMENTS

2.2.1. VOC MEASUREMENTS

A custom-built online multichannel gas chromatograph (GC) was used to measure a suite of 46 VOCs (Abeleira et al., 2017). The sampling inlet was 6m above ground level (a.g.l.). Measurements were taken about every forty minutes for both spring and summer datasets. Data from the spring and summer datasets represents merged data waves. The values are averaged over a ten-minute period corresponding to 5 minutes before and five minutes after the measurement timestamp. All VOC measurements are reported in mixing ratios. For additional information on the GC instrument used in this study, including limits of detection for each VOC measured, please reference Abeleira et al (2017).

2.2.2. TRACE GAS MEASUREMENTS

A suite of 11 reactive trace gases were co-measured along with the VOCs. Carbon monoxide (CO) and methane (CH_4) were measured with a commercial Cavity Ring-

Down Spectrometer (Picarro 6401) (Abeleira et al. 2017). Carbon monoxide and CH_4 were measured at ~3 second intervals. The data was then averaged for ten minutes centered on the VOC timestamp.

Nitric oxide (NO) and NO_2 were quantified using the chemiluminscence technique with a Teledyne Model 200EU. Each nitrogen species was measured in situ then compiled to make the NO_x and NO_z measurements that together make up NO_y. The NO_2 mixing ratio was calculated by subtracting ambient NO from the NO_2 mixing ratio after NO_2 was selectively converted to NO using a blue-light photolytic converter (Air Quality Designs, Inc.) (Abeleira et al. 2017). NO_y is the sum of NO_x (NO and NO_2) and NO_z (HNO_3, PAN, HONO, organic nitrates, and other reactive nitrogen species). Peroxyacetyl nitrate (PAN) was measured with the custom-built NCAR GC-ECD (Flocke et al., 2005). For more information on non-VOC measurements at BAO during this dataset, please refer to Lindaas (2017).

A 2B Technologies O_3 monitor (Model 202) was used to measured O_3 mixing ratios. The trace gas measurements were merged over one minute before being merged again over the same ten-minute period as the VOC data. Additional information on the trace gas measurements can be found in Lindaas et al. (2017).

2.2.3. METEOROLOGICAL MEASUREMENTS

Meteorological data, including wind speed and direction, temperature, and relative humidity made, were measured in situ at 10m a.g.l. The meteorology station was attached on the south side of the BAO tower. Wind directions were corrected to account for the eddy of the tower with northerly winds. Calculations for absolute

humidity are taken from *Humidity Conversion Formulas* (Vaisala, 2013). Meteorological measurements were merged over ten minutes about every forty minutes.

2.3. TREATMENT OF DATA

Data was recorded during the summer from 5 July to 6 September 2015. Summer measurements were restricted twice. The data before July 11 and after August 15 were impacted by aged wildfire smoke. Valid VOC measurements were further restricted by water in issues in the GC system during the first weeks of July. The summer data was therefore restricted to July 24 – August 14.

We identify periods of data contusive to photochemical MEK production using the following criteria: We required that PAN is two standard deviations above average (> 500 pptv) during peak daytime hours (10:00-16:00). PAN is a sensitive indicator of photochemistry. It typically has low background mixing ratios, and it is not emitted directly (Fischer et al., 2014). PAN is formed by the oxidation of a wide array of non-methane volatile organic compounds (NMVOCs) in the presence of NO_x (Stephens, 1969; Fischer et al., 2014). PAN can be transported long distances, and when it thermally decomposes, it releases NO_x and can trigger O_3 production far from the original NO_x source (Singh and Hanst, 1981; Fischer et al., 2014). The lifetime of PAN against thermal decomposition, its primary loss pathway in the troposphere above the surface, is a strong function of temperature (Fischer et al., 2014; Singh et al., 1987). The lifetime approximately doubles for each 4C° drop in temperature (Singh et al., 1987).

2.4. HYSPLIT TRAJECTORY CLUSTERS AND ANALYSIS

We used a backward trajectory analysis to determine the origin of air masses during the spring and summer (Draxler & Hess, 1998). We ran 72-hour back-trajectories originating at the BAO. The trajectories started at 2000m A.G.L. so that the trajectories were less influenced by the complex dynamics of the Rocky Mountains. The trajectories were then clustered by a k-means cluster analysis. The k-means analysis clustered each trajectory into a predetermined number of clusters by minimizing the distance between each trajectory and its nearest neighbor; this technique has been used to examine air mass movement in previous studies (Moody et al., 1998). The k-means analysis was able to cluster 66% of the trajectories. The remaining 34% of data (169 trajectories) were truncated from the dataset when they intersected the ground. For more information on the HYSPLIT trajectory clusters, please reference Lindaas et al. (2017).

2.5. BOX MODEL

We used a chemical box model to determine how individual precursors affect the mixing ratios of MEK. The chemical mechanistic information was taken from the Master Chemical Mechanism, MCM v3.2. The MCM is a near explicit chemical mechanism, which describes the gas-phase chemical processes involved in the atmospheric degradation of primary emitted VOCs, including OVOCs (MCM). The height of the simulations was set to 1 km A.G.L. and the ambient temperature was set to 300K. The model does not take into account effects of deposition, turbulent mixing, or entrainment/dilution (Lindaas,

2017). Each simulation was run for 8 hours at ten-minute time steps. A full list of parameters can be found in Lindaas (2017)

The initial values for the baseline box model run were the measured median summer mixing ratio for each chemical species measured at the BAO. We conducted a series of additional simulations where we increased initial mixing ratio of each of the three MEK precursors (n-Butane, i-Pentane, and 3-Methylhexane) individually by 10%, allowing us to quantify the effects of individual precursors on MEK production.

3. RESULTS

3.1. DATA SUMMARY

3.1.1. SEASONALITY

Generally, we observed higher mixing ratios of MEK in the summer data set than in the spring data set as shown in Figure 2 and Tables 1 and 2. Figures 2a and 2b show MEK mixing ratios throughout spring and summer, respectively.

Tables 1 and 2 examine the descriptive statistics for MEK, source tracers, and precursors in spring and summer, respectively. Mixing ratios of MEK in spring were significantly lower ($p << 0.001$) than summer MEK (Figure 3). While mixing ratios of n-butane and i-pentane were also lower in spring, mean mixing ratios of spring 3-methylhexane increased by more than 50% compared to summer. The maximum mixing ratio of 3-methylhexane in spring was almost double the maximum mixing ratio in summer. The mean spring mixing ratio of PAN was slightly higher than that of summer PAN but the maximum summer PAN was approximately double spring

maximum. Spring CO was significantly elevated relative to summer CO ($p << 0.001$) but the spring maximum CO peaked at more than double summer CO.

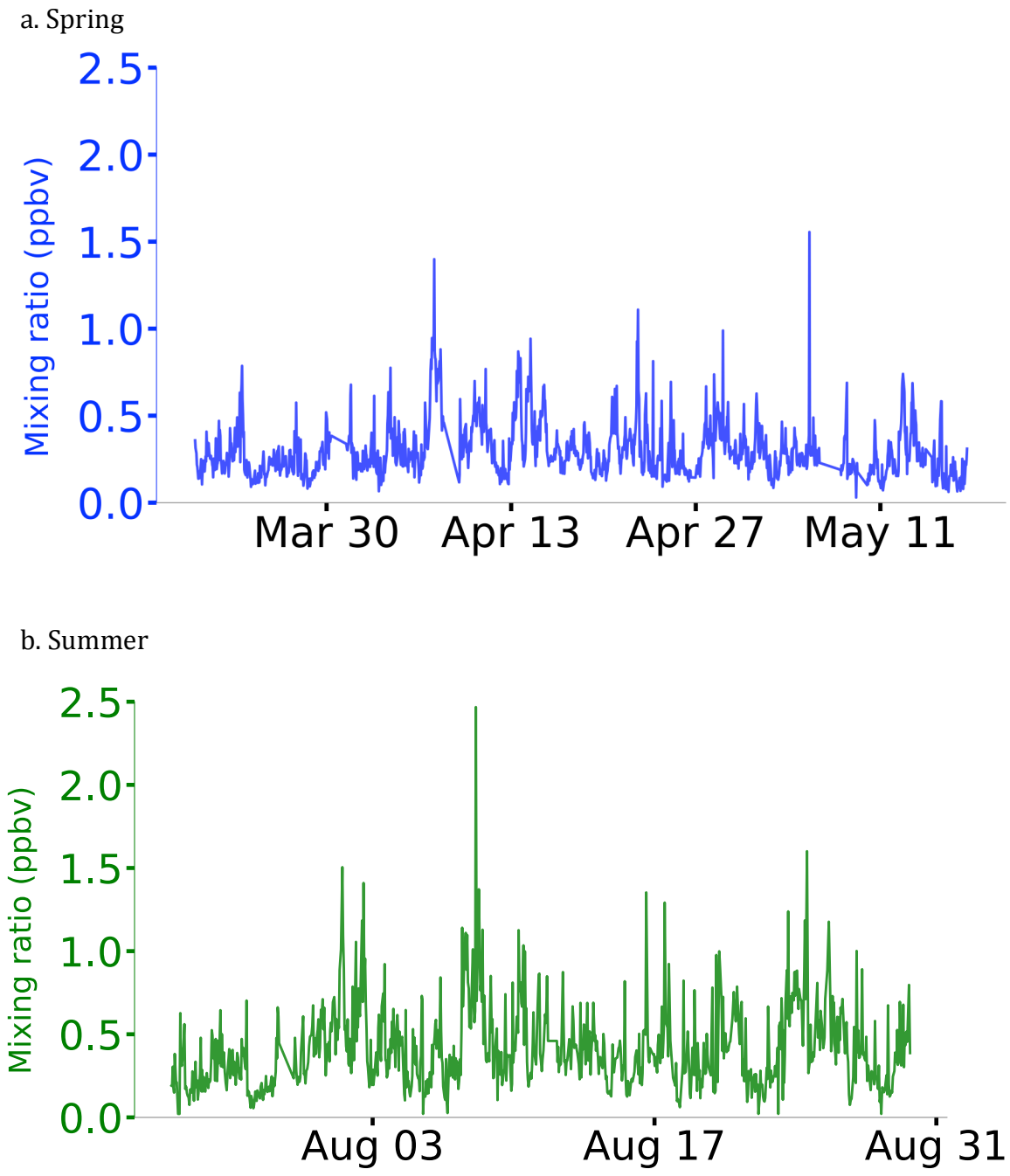

Figure 2. MEK measurements from BAO in (a) spring and (b) summer 2015.

Table 1: Table of descriptive statistics from spring 2015. All values are in ppbv unless otherwise noted.

	Mean	Max	Min	Standard Dev.	N
MEK	0.297	1.56	0.03‡	0.157	1341
n-butane	1.90	58.8	0.0015‡	3.42	1341
i-pentane	1.13	61.7	0.0015‡	2.61	1341
3-methylhexane	0.147	2.55	0.01‡	0.204	1341
Ethyne	0.226	1.27	0.053	0.124	1341
PAN*	202.8	763.0	51.0	103.5	1158
CO	156.2	661.5	101.7	37.27	1134

*PAN measured in pptv.

‡Indicates the minimum value was below LOD. See Abeleira et al. (2017) for treatment of values below LOD.

The mean summer MEK mixing ratio falls into the wide range of global MEK measurements (Yañez-Serrano et al., 2016) which range from 0.02 ppbv in remote regions (Singh et al., 2004) to ~15 ppbv in areas heavily influenced by heavy traffic and urban emissions (Grosjean and Swanson, 1983). The precursor species were consistently elevated at the BAO. The mean summer mixing ratio of n-Butane was higher relative to Los Angeles and Salt Lake City (Baker et al., 2008). The mean summer mixing i-pentane was also elevated compared to Los Angeles and Salt Lake City. Mixing

ratios of ethyne, PAN, and CO at BAO were lower relative to other urban areas across the US (Baker et al., 2008).

We used a two tailed t-test of equal variance to examine the significance of differences between the summer and spring data. We found that there was a significant difference at the 95% confidence interval between spring and summer for all species except for PAN ($p = 0.078$) and ethyne ($p = 0.39$).

Table 2. Table of descriptive statistics from summer 2015. All values are in ppbv unless otherwise noted.

	Mean	Max	Min	Standard Dev.	N
MEK	0.407	2.47	0.03‡	0.250	533
n-butane	3.80	78.2	0.023	5.67	533
i-pentane	2.93	82.2	0.0015‡	4.94	533
3-methylhexane	0.0847	1.26	0.01‡	0.121	533
Ethyne	0.242	2.09	0.003‡	0.168	533
PAN*	195	1462	42.5	140	523
CO	131.4	291.4	70.3	31.0	517

*PAN measured in pptv.

‡Indicates the minimum value was below LOD. See Abeleira et al. (2017) for treatment of values below LOD.

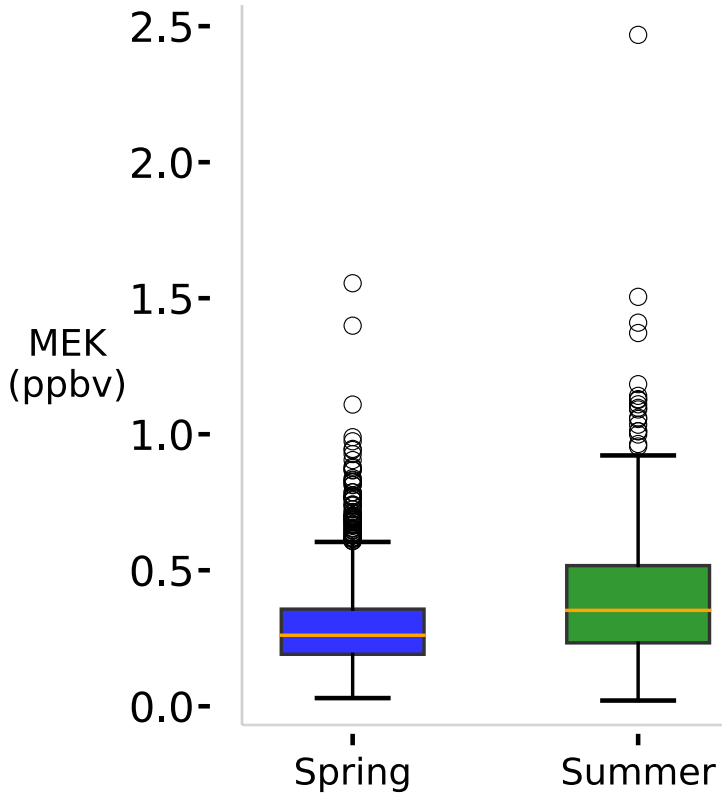

Figure 3. MEK distributions from spring and summer. The orange line within the boxplots represents the median value for both seasons, respectively.

3.2. DIRECTIONAL DEPENDENCE

3.2.1. MEK

We used the meteorological and VOC data to create a "pollution rose" in order to examine if a given wind speed and direction were associated with higher mixing ratios of a species compared to others. These pollution roses allow us to investigate the directional dependence of MEK mixing ratios. Both spring and summer had elevated MEK with northerly and easterly winds ($p << 0.001$ for both seasons). During spring, MEK had elevated mixing ratios from the E and NE (Figure 4). Easterly winds (45°NE-135°SE) had the highest mean MEK (0.328 ppbv). Northerly (315°NW-45°NE) winds

had a mean MEK mixing ratio of 0.305 ppbv but with the fewest observations (N = 242). Southerly winds (135°SE-225°SW) had a mean MEK mixing ratio of 0.263 ppbv. Westerly winds (315°NW-225°SW) had the lowest mean MEK (0.263 ppbv) but the most observations (N = 394).

During summer, MEK did not have a clear directional dependence. We observed the highest mean MEK (0.467 ppbv) but the fewest observations (N = 59) with northerly flow. Easterly and westerly flow had similar mean mixing ratios (0.415 ppbv and 0.412 ppbv, respectively). Southerly winds had the lowest mean MEK (0.376) but the most observations (N =187).

From this point forward we focus solely on the summer because the objective of our work is to fully characterize when MEK was produced by photochemistry. Generally, we would expect less photochemistry in spring than summer and is more heavily influenced by direct emissions of MEK. Focusing on summer allowed us to better distinguish elevated levels of MEK that were produced by photochemical activity from those that were not. This separation will allow us to better understand the data that were not explained by photochemistry. We also set out to begin to classify and quantify other sources of MEK during summer that were not explained by the PMF solution from Abeleira et al (2017) in order to better understand the effect of photochemistry on OVOC abundance in the NFRMA.

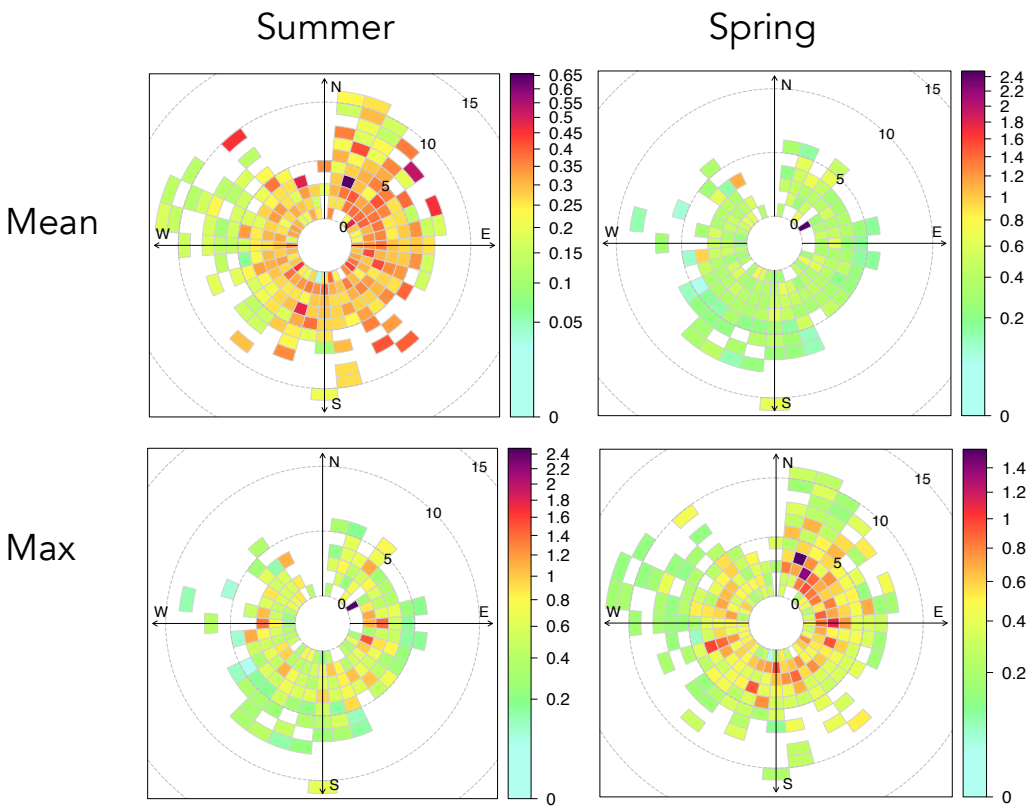

Figure 4. Polar frequency plots (pollution roses) of mean and maximum MEK during spring and summer 2015. Wind observations are binned by 10° wind direction and 1.0 m/s^{-1} wind speed. The bins are then colored by mean mixing ratio (ppbv) for each bin. Note the difference in scales between seasons and statistic in order to show the variability.

3.2.2. MEK PRECURSORS

The suite of VOCs measured in this study includes three known precursors for MEK: 3-Methylhexane, n-Butane, and i-Pentane (Sommariva et al. 2011). Figure 5 shows that all three precursors had maximum mixing ratios associated with moderate easterly winds (from 270° at 2 m/s). These three precursors also had higher mean

mixing ratios from the north. The highest mean values for all three precursors were from the NE and NW with mild wind speeds (1 m/s). The direction and wind speed with the highest mean mixing ratios of precursors (45° NE @ 1 m/s) was the same combination during the highest mean and max mixing ratios of summer MEK. While the highest mean mixing ratios are associated with NE winds, the highest maximum mixing ratios came with moderate winds from the west. The highest mixing ratios for all three precursors were associated with 3 m/s wind from due west.

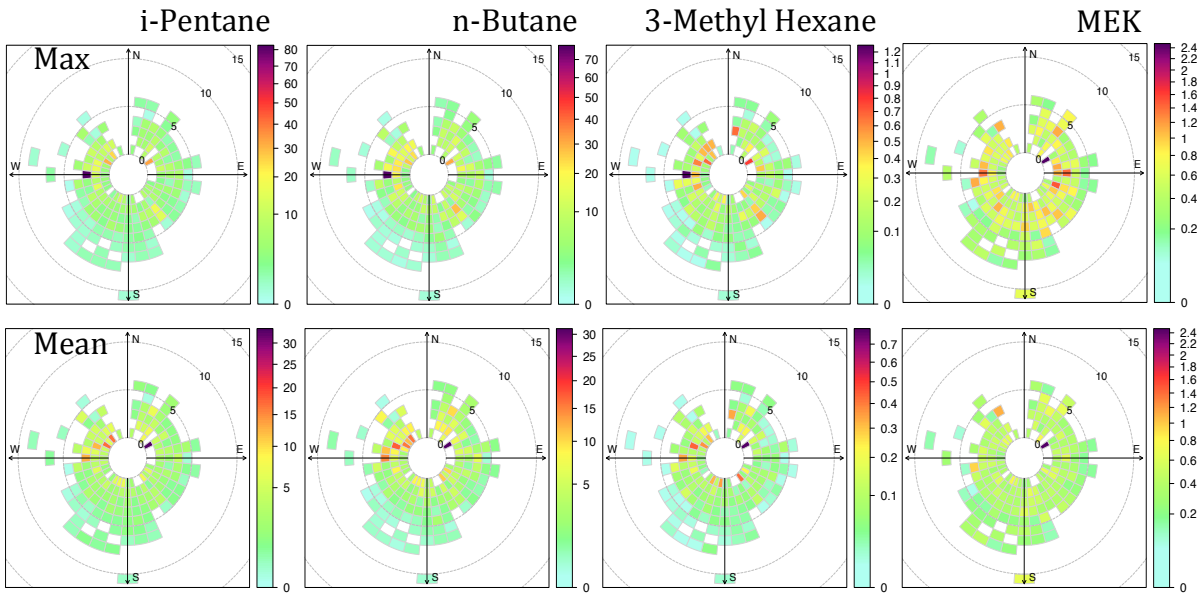

Figure 5. These polar frequency plots are binned by wind speed at a given direction then colored by the maximum and mean mixing ratios (in ppbv) of each bin for summer 2015. Note the different scales for each statistics and compound.

3.2.3. EMISSION SOURCE TRACERS

We selected four source tracers to examine the different air masses that affect the study site. We used the same tracers set by Abeleira et al. (2017): ethyne as an

indicator of vehicle traffic emissions, carbon monoxide (CO) as an indicator of urban emissions, and propane as an indicator of emissions from ONG production (Figure 6). We used benzene as an additional indicator of emissions from oil and natural gas (Halliday et al, 2016). Overall, the directional dependence of the chosen source tracers was consistent with our understanding of emission sources in the NFRMA. For example, ethyne shows increased emissions from the west and east, which was consistent with motor vehicle emissions from nearby I-25, a major thoroughfare of the Front Range (Figure 1). The increased emissions from the south are likely emissions from the suburban areas around Denver and Boulder, or from the cities themselves. The pollution rose for CO shows increased mixing ratios from the S and W, indicating emissions from the urban centers in those directions (Denver and Boulder, respectively). The pollution rose colored for maximum mixing ratios in each bin indicates there are significant emissions from the S, most likely from the Denver Metro Area. Oil and natural gas extraction activity likely dominates the local emission of light alkanes in the Front Range (Abeleira et al., 2017). Abeleira et al. (2017) similarly found that the elevated quantities of light alkanes are likely a major source of MEK in the Front Range.

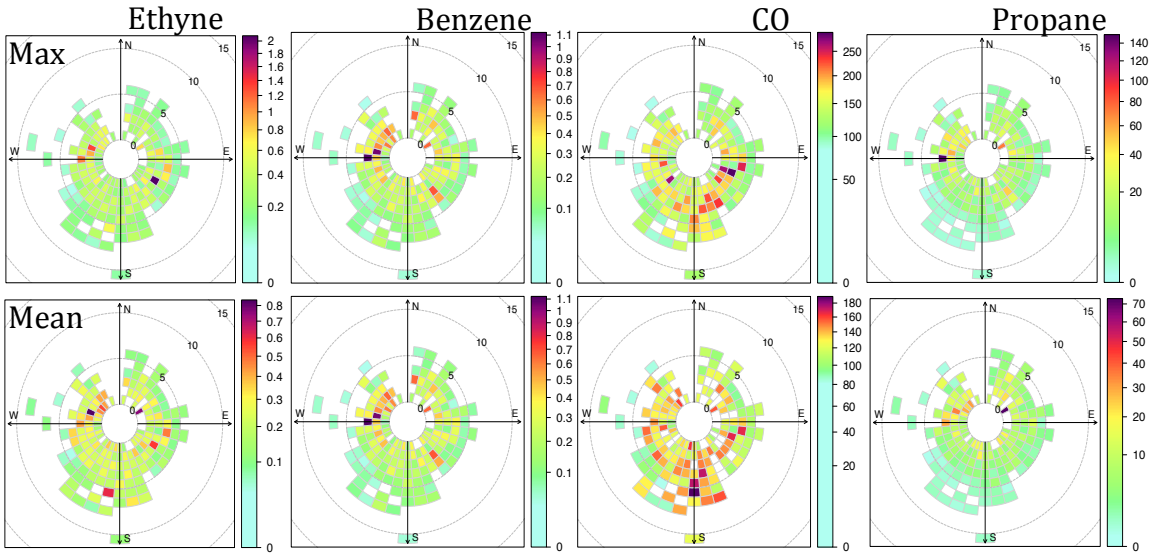

Figure 6. Plots are binned by 10° wind direction and by 1 ms^{-1}. Wind speed and direction bins are colored by maximum and mean mixing ratios (ppbv), respectively.

3.3. PHOTOCHEMICAL RELATIONSHIP

There were eight days that fell into our active photochemistry metric from the summer data set (Figure 7). Our photochemistry case study (Figure 10b) agreed with this metric. The average MEK value during these eight photochemical events was 0.84 ppbv, more than double the average mean for the entire MEK dataset. Our conservative photochemistry metric resulted in photochemistry during 36% of days in the summer dataset. If the metric was loosened to when PAN was above 350 pptv (one standard deviation above the mean) we found that 59% of days during the summer dataset (13 days) had evidence of active photochemistry.

During active photochemistry hours (10:00-16:00), we find a weak relationship between MEK and PAN ($R = .154$, $p = 0.0813$). The relationship was stronger in the late morning and early afternoon (10:00-13:00; $R = .536$, $p << 0.001$) than in the early to late

afternoon (13:00-16:00; R =.149, p =.239). Increased afternoon cloud cover could cause this decrease in late afternoon photochemistry from the Colorado Monsoon that lowers solar insolation. Interestingly, we found a relatively strong relationship between MEK and PAN (R = 0.334, p = 0.004) during the early morning hours (7:00-10:00). During this time, PAN was low (due to lack of photochemistry in morning hours) and MEK was elevated. Morning MEK could be elevated because of an unexplained path of formation, such as a direct emission source, transport, or from rapid mixing of air from aloft.

The time series of MEK and PAN show when MEK was produced by photochemical oxidation and when it was not (Figure 7). MEK and PAN generally follow each other throughout the summer but there are days when they do not share the same diurnal pattern. These data cannot be explained by photochemical production and the mixing ratios must be explained by another source. We explore these two different scenarios using two case studies that show each production mechanism clearly.

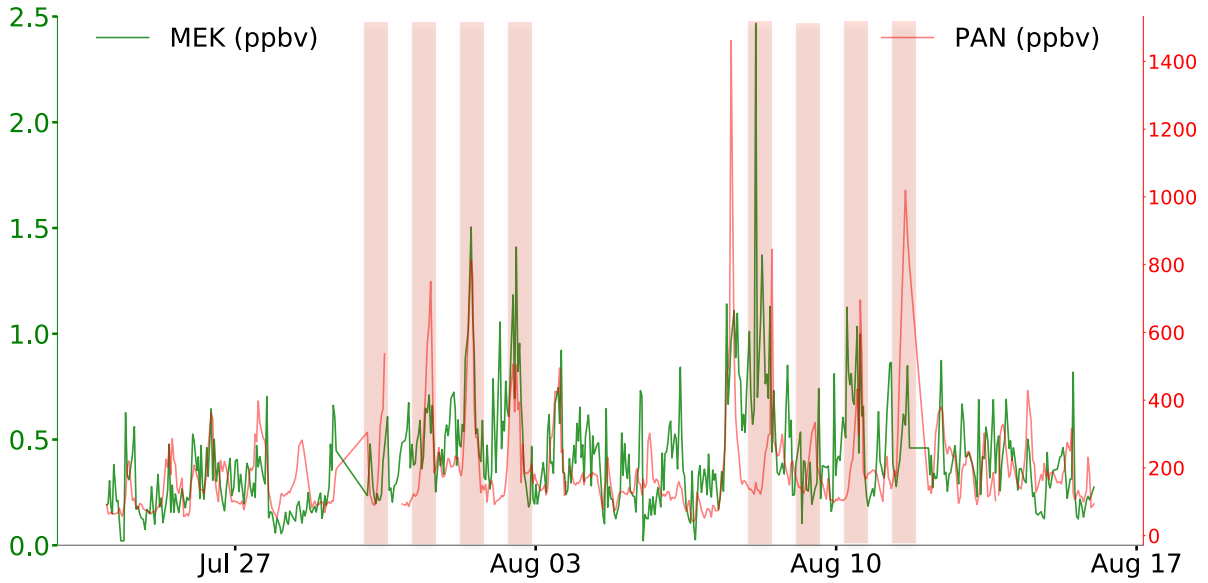

Figure 7. Time series of PAN (blue) and MEK (red) during the summer dataset. Cases that meet our photochemistry metric are shaded in red.

3.3.1. CASE STUDIES

We selected two one-day periods to look more closely at MEK enhancements during periods of active photochemistry (August 1) and during diminished photochemical activity (August 6). August 1 fell under the photochemistry metric we applied to the summer dataset while August 6 did not. We saw on August 1 that both MEK and PAN rise in the late morning before falling in the late afternoon. The two species shared a very similar pattern throughout the course of the day. We saw something very different on August 6. When MEK began to rise throughout the day, PAN did not similarly increase. The amount of PAN varied little throughout the day and remained below 150 pptv.

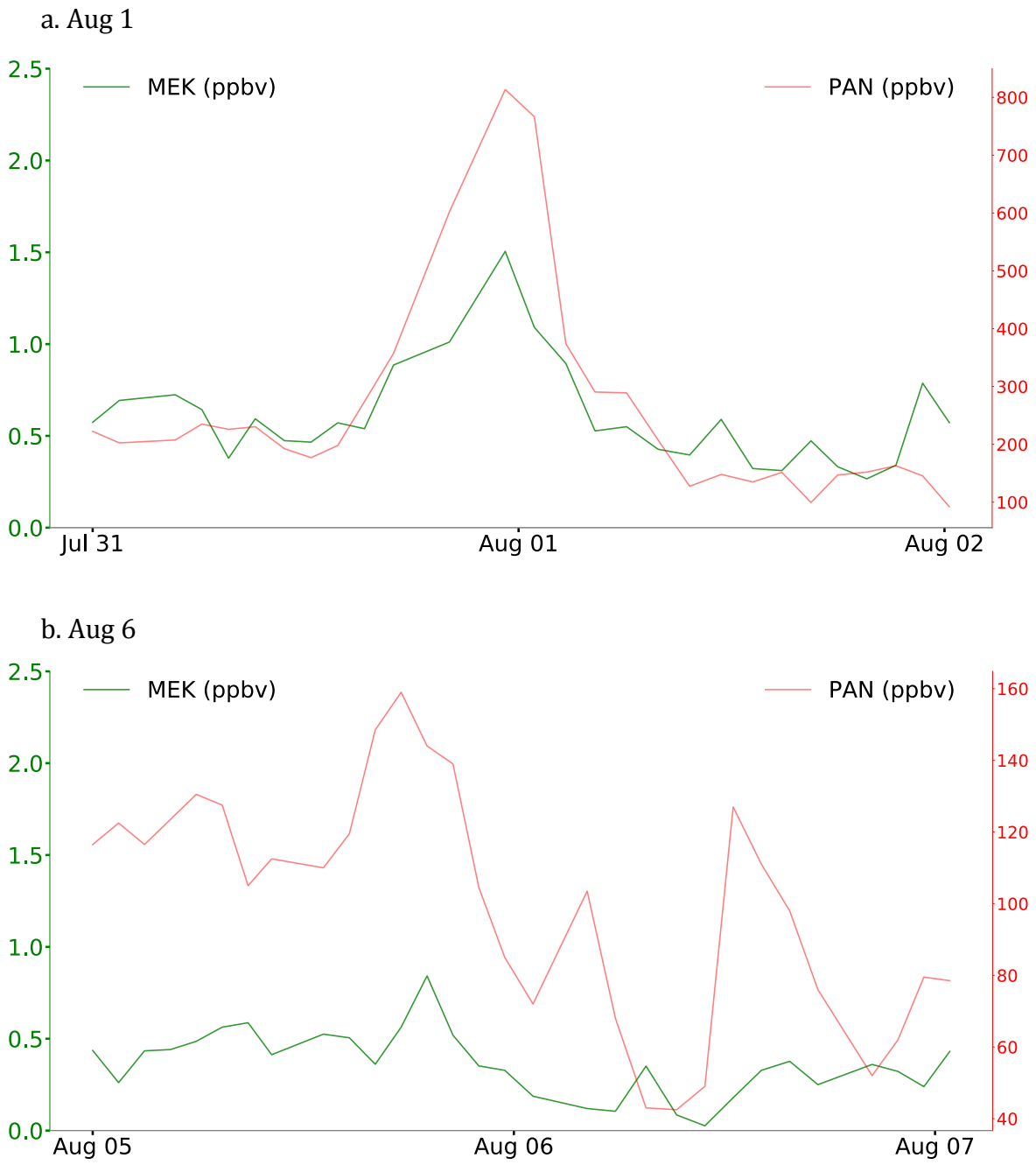

Figure 10. Our case studies for days with a) strong evidence of MEK photochemistry and b) no evidence for MEK photochemistry.

3.3.2. DIURNAL PROFILE

When the high photochemistry days are separated out, a diurnal pattern begins to emerge. We extracted the values from days given by the photochemistry metric then averaged the values by the hour the data were measured (Figure 8). This pattern shows a defined peak of MEK during peak photochemistry hours and decreasing mixing ratios further from the photochemical peak. The mean daytime MEK (0.68 ppbv) for these high photochemistry days was significantly higher ($p << 0.001$) than mean daytime MEK from the rest of the summer (0.49 ppbv). There are two peaks in the early morning that correspond to some of the highest MEK values from the summer. As the sun was not out at 5am, the mechanism behind these values cannot be explained by photochemistry and must therefore be attributable to a direct source emission or other chemical formation pathway.

When the days selected by our photochemistry metric were compared to the rest of the days from summer 2015, the diurnal cycle of MEK photochemistry becomes more apparent. Days that did not meet our photochemistry metric show peaks in the morning (8am) and in the evening (3 & 5 pm). These times corresponded well with peak rush hour times (Harley et al., 2005) in the NFRMA. These peaks suggest that MEK was directly emitted from vehicle exhaust. During active photochemistry days, those times generally correspond with lower mixing ratios of MEK. Abeleira et al. (2017) found that traffic-related emissions contributed little to VOC reactivity during summer 2015 in the NFRMA. We note that there are no observations of MEK emissions from

tailpipe emissions (Yañez-Serrano et al., 2016) although vehicle exhaust is a direct emission source for other closely related OVOCs (Bon et al., 2011; Brito et al., 2015).

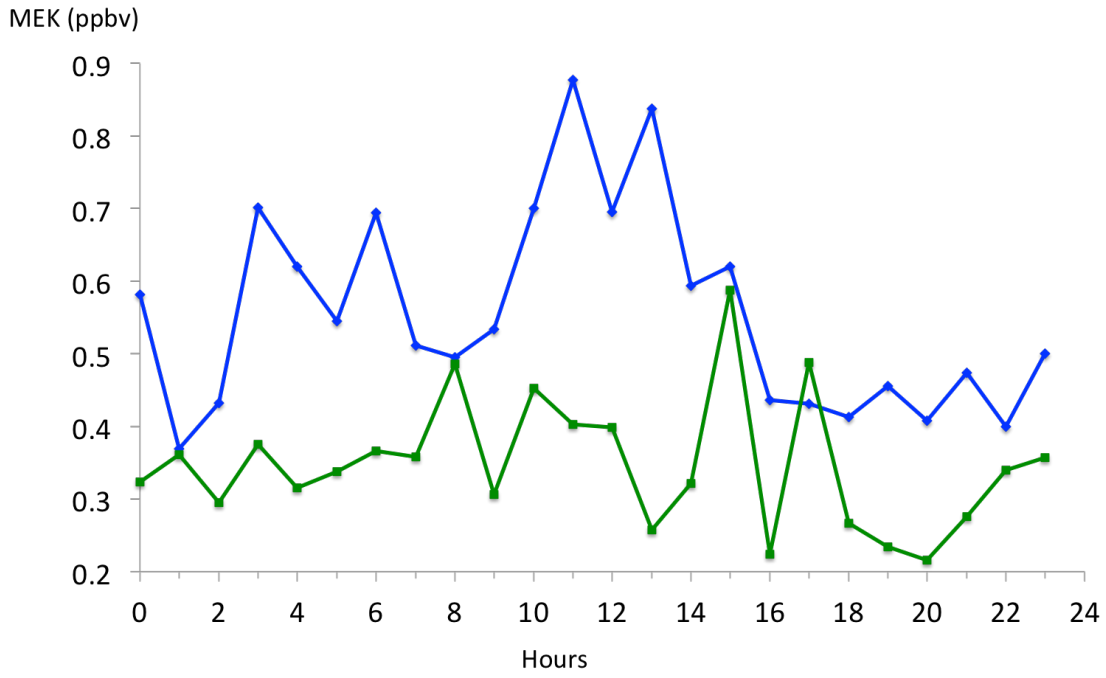

Figure 8. Average diurnal cycle of MEK for days with that meet our photochemistry metric (blue) compared to days that did not meet the photochemistry metric (green).

3.3.3. SPECIES CORRELATIONS

We computed correlation coefficients for MEK and the other gases measured during this campaign. We found that the highest correlations during summer were between MEK and the alkyl nitrate species ($R > 0.4$). The other OVOC species were also positively correlated with MEK ($R = 0.43$-0.49, $p << 0.001$). MEK was not strongly correlated in summer with known precursors or tracers of urban/traffic emissions ($R = 0.35$-0.39, $p << 0.001$) and was negatively correlated with CO ($R = -0.12$, $p = 0.008$). A stronger diurnal correlation emerged when the precursors were compared to MEK by

time of day (e.g. during peak photochemical hours v.s. not peak p. Generally, the precursors were more positively correlated with MEK during the daytime hours (10:00-16:00) (Table 3). During the most active photochemical hours, we found MEK was most strongly correlated with n-butane (R = 0.56) and PAN (R = 0.56). We found that MEK was most highly correlated with ethyne (R = 0.44) and n-butane (R = 0.44) during hours that are not characteristically associated with high photochemistry. The tracers of urban and combustion emissions, ethyne and CO, are highly correlated during both time periods.

Table 3. This table shows Pearson Correlation coefficients for summer 2015. Values in bold are significant to the .05 level. Values in red and bold are significant to the .01 level.

		MEK	n-Butane	Ethyne	PAN	CO
Non-Peak Photochemistry Hours (16:00 – 10:00)	MEK	-	**.44**	**.44**	**.30**	**.28**
	n-butane	-	-	**.61**	.02	**.12**
	ethyne	-	-	-	**.20**	**.57**
	PAN	-	-	-	-	**.24**
	CO	-	-	-	-	-
Peak Photochemistry Hours (10:00 – 16:00)	MEK	-	**.56**	**.27**	**.56**	**.52**
	n-butane	-	-	**.30**	**.64**	**.57**
	ethyne	-	-	-	**.23**	**.56**
	PAN	-	-	-	-	**.77**
	CO	-	-	-	-	-

We compared MEK to PAN in order to further examine the relationship with photochemistry (Figure 9). The data are color-coded by hour of day. There was a weak positive relationship between PAN and MEK during all hours of the day (R = 0.0764, p =

0.0778). We found a positive relationship between MEK and PAN (R = 0.154, p = 0.0813) during peak photochemistry hours (10:00-16:00). The relationship between MEK and PAN was strongest (R = 0.535, p << 0.001) during the late morning and early afternoon (10:00-13:00). Late afternoon MEK (13:00-16:00) has a weaker relationship with PAN (R = 0.1447, p = 0.239). Methyl ethyl ketone has a variety of chemical pathways that are active during photochemistry. The variations in responsiveness to photochemistry may be connected to shifts in production mechanisms or atmospheric conditions.

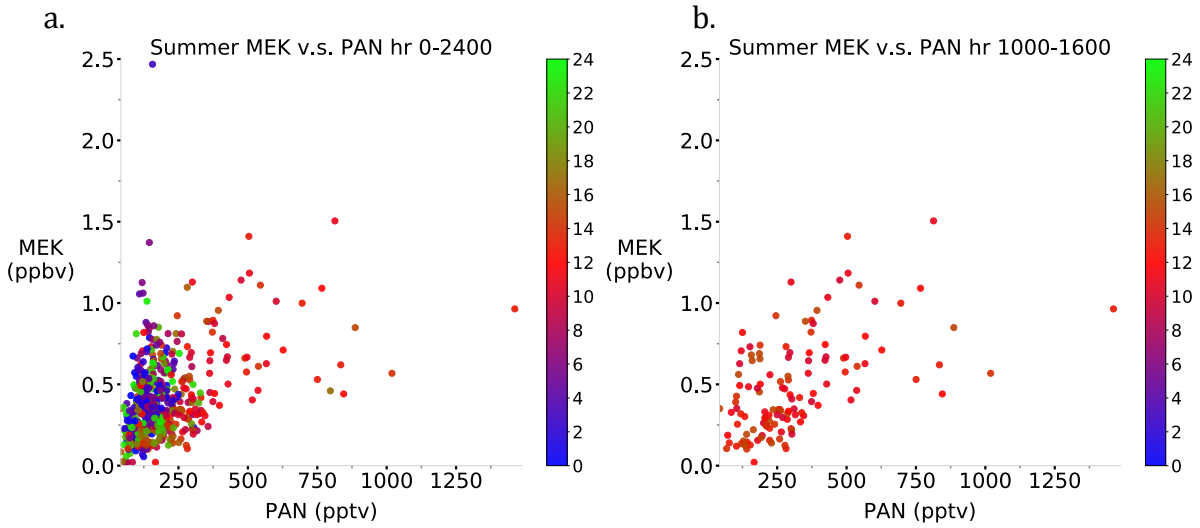

Figure 9. These scatter plots show MEK plotted against PAN and colored by hour during a) all hours of the day and b) during peak photochemistry hours (10:00-16:00)

3.4. TRAJECTORY CLUSTERS

Cluster 1 represents synoptic scale transport from the WNW. Cluster 2 is stagnant or uncertain conditions around the BAO site. Cluster 3 shows short-range

transport from the SW while Cluster 4 represents long-range transport from the SW (Figure 11).

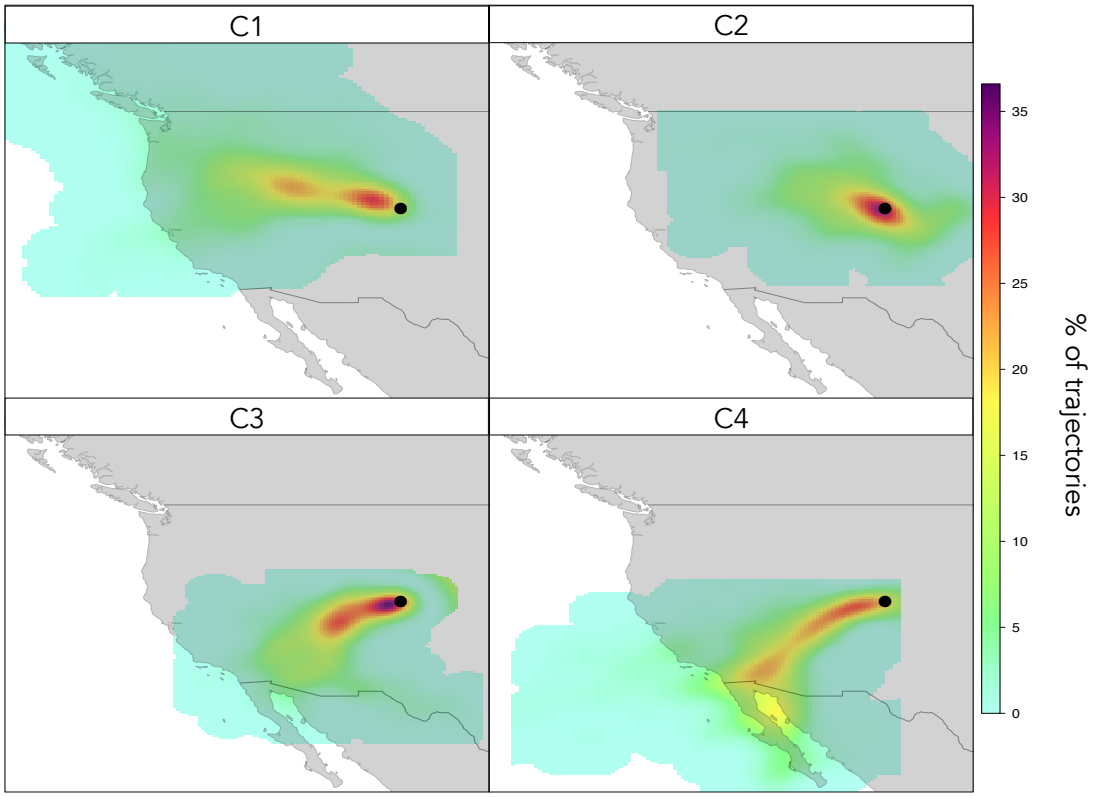

Figure 11. 72-hour HYSPLIT back trajectory analysis from the BAO during summer 2015 (Lindaas, 2018).

The highest mixing ratios of MEK were measured in Clusters 2 (C2) and 4 (C4) (Table 4). C2 had the highest average mixing ratios of both CO and PAN. C4 had the highest average mixing ratios of known precursors, ONG tracers, and vehicle tracers. The average mixing ratio of n-butane was highest in the sub-set classified as C4 (Table 4). These max values were several orders of magnitude higher than the next highest cluster. The maximum values for propane, n-butane, and ethyne were 2 times higher

than the maximum values of next highest cluster (C2). The increase in ONG and traffic tracers likely showed the accumulation of those tracers when air movement, and therefore transport, was reduced. We expected to see higher mixing ratios of ONG and traffic tracers because of the proximity to both the Denver Metropolitan Area and WGF.

We split the measurement data by cluster and applied a similar correlation analysis to each cluster as was applied to the whole dataset (Table 4). When divided by clusters, we found a relationship between trajectories and mixing ratios of MEK. C2 had the highest overall MEK ($p = 0.17$), though the precursors are not as strongly correlated as in other clusters. Instead MEK is correlated strongly with PAN and CO in C2. There was a higher correlation between MEK and the precursors when we had longer-range transport of air masses (C1, C3, and C4).

Table 4. Table of the descriptive statistics broken down by cluster for MEK, n-butane, and select source tracers for summer 2015. Bold values are the highest values for each species.

Cluster number		Mean	Maximum	Minimum	Std. Deviation	N
1	MEK	0.320	0.653	0.026	0.153	55
	n-butane	2.73	11.8	0.083	2.566	55
	ethyne	0.223	0.596	0.056	0.129	55
	CO	132.1	**291.4**	83.4	32.7	55
	PAN	168.2	536.5	42.5	99.6	47
2	MEK	**0.438**	1.18	**0.126**	0.202	106
	n-butane	2.93	36.4	0.214	4.78	106
	ethyne	0.264	0.856	**0.070**	0.145	106
	CO	**144.5**	246.8	96.8	30.03	100
	PAN	**255.4**	1019.0	**86.0**	171	105
3	MEK	0.390	1.13	0.125	0.187	90
	n-butane	3.63	19.4	**0.198**	3.86	90
	ethyne	0.215	0.773	0.059	0.126	90
	CO	121.0	193.5	**85.7**	25.3	89
	PAN	173.0	315.5	56.5	69.8	89
4	MEK	0.393	1.37	0.055	0.263	113
	n-butane	**4.68**	**78.2**	0.117	8.31	113
	ethyne	**0.274**	**2.09**	0.043	0.259	113
	CO	131.6	268.4	70.3	37.0	112
	PAN	174.3	**1461.5**	52.0	168.0	113

3.5. BOX MODEL

We used the BOXMOX chemical box model to examine which precursors MEK formation is most sensitive to over an 8-hour period. We find that a 10% increase in n-butane above the observed median value results in the largest increase (3.74%) of MEK mixing ratios compared to the baseline run. Increases in 3-Methyl Hexane and i-Pentane did not increase MEK significantly (0.025% and 0.051%, respectively) and remained very close to the baseline run (see inset to Figure 12) over the 8-hour integration period.

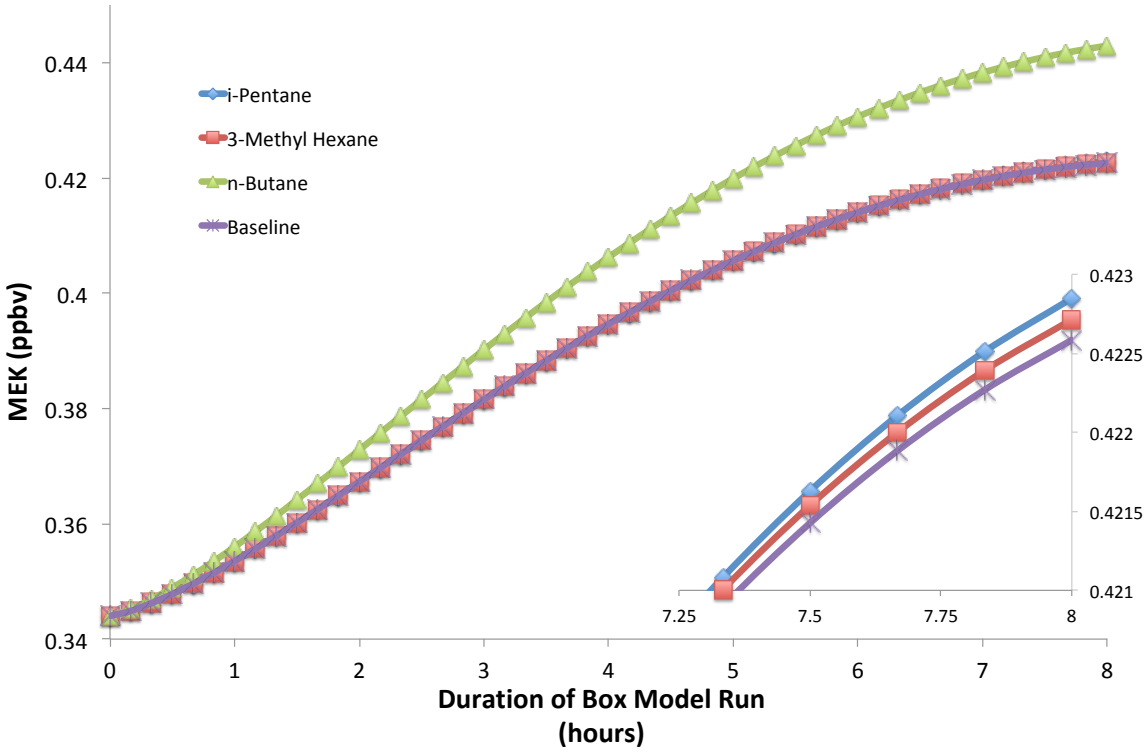

Figure 12. Box model outputs when there is a 10% increase in each precursor. The inset shows the last 45 minutes of the box model run where i-Pentane and 3-methylhexane separate from the baseline run.

4. DISCUSSION

Our observations lead us to conclude that light alkane emissions from ONG production and extraction in the Wattenberg Gas Field contributed to the secondary photochemical production of MEK in the NFRMA region. We found a strong relationship between mixing ratios of propane, a known marker of natural gas extraction (Petrón et al., 2012), and n-butane ($R = 0.99$, $p << .001$), indicating the importance of the WGF as an emission source of n-butane in the Front Range. The photochemical oxidation of n-butane was previously found to be one of the dominant precursors for MEK production (Formula 1), accounting for 20-30% of MEK during the NEAQS (Sommariva et al., 2011). The high mixing ratios of n-butane in the NFRMA combined with the high yield of MEK from n-butane, as shown in our box model, suggests that this is a dominant mechanism for secondary photochemical production of MEK at BAO during summer 2015.

We also saw elevated mixing ratios of light alkanes at BAO, specifically n-butane. The prevalence of these hydrocarbons showed that the air mass present at BAO was more heavily influenced by the emissions of these alkanes than urban emissions from the nearby Denver Metro Area (Abeleira et al., 2017). Abeleira et al. (2017) found the VOC reactivity at BAO was more similar to semi-rural areas in close proximity to natural gas operation (e.g. Hickory site, Pennsylvania [Swarthout et al., 2015]) than other well-studied urban areas. We found that the amount of n-butane at BAO was comparable to other natural gas production areas (Marcellus shale, [Swarthout et al., 2015]; Anadarko Basin, [Katzenstein et al., 2003]). Our findings supported the findings of Abeleira et al.

(2017) that ONG activities in the region influenced both primary VOC mixing ratios and the atmospheric oxidation chemistry of the region.

We used the BOXMOX output to explicitly quantify the importance of n-butane to the secondary formation of MEK. Of the precursors that were measured at BAO and examined with BOXMOX, n-butane was the dominant precursor (yield = 46%). We found that a 10% increase in n-butane was significantly different from the baseline output at a 95% confidence level (paired 2-tailed t-test, $p << 0.001$). We similarly found strong evidence for the dominance of MEK production by n-butane photochemical oxidation during our active photochemistry case study (August 1, Figure 10a). We found a significant relationship during all hours of the day between MEK and PAN ($R = 0.86$, $P << 0.001$), as well as a significant relationship between n-butane and MEK ($R = 0.54$, $p = .003$). Our finding that the photochemical oxidation of n-butane is likely the dominant pathway for secondary MEK production is consistent with the findings of Sommariva et al. (2011) and Singh et al. (2004).

While the photochemical oxidation of n-butane is an important source in the NFRMA, we have identified periods of elevated MEK that do not occur during periods of active photochemistry. Therefore, we postulate that there are important unexplained sources of MEK. During our case study (August 6, Figure 10b) with little to no photochemistry, we still found MEK and n-butane to be closely correlated. Interestingly, we found August 6 had a significant correlation between MEK and n-butane ($R = 0.47$, $p = 0.013$) as to what we observed on August 1, although photochemical activity was very low, given the low PAN mixing ratios. Further, we saw a delay between n-butane peaks and subsequent MEK peaks throughout the day. While Abeleira et al. (2017) suggested

that the photochemical oxidation of n-butane was likely a major source of MEK in the NFRMA, this significant correlation occurred in the presence of low photochemistry and we cannot explain the dominant mechanism of MEK production during this case study.

There are several possible explanations for periods of elevated MEK in the absence of photochemical activity. This relationship could appear if there were another precursor similar to n-butane (e.g. i-pentane, 3-methyl hexane, etc.) that is being oxidized in the atmosphere; however, given that there is no photolytic production of OH, the primary atmospheric oxidizer of VOCs, this is unlikely (Mellouki et al., 2015). Alternatively, if these mixing ratios were a result of oxidation of precursors, it is possible that another oxidation agent, such as nitrate, could be reacting with precursors or other unsaturated oxygenated species (Mellouki et al., 2015). It is also possible that MEK is being directly emitted from areas with high emissions of light alkanes. Many of the unconventional natural gas extraction methods use proprietary chemical recipes and chemical storage techniques that could be a source of primary OVOCs or precursors (Adgate et al., 2014; Halliday et al., 2016)

Another potential source could be the transport and formation of MEK in moist air masses. Rodigast et al. (2016) detected significant amounts of MEK in cloud water, ice and rain. MEK was also found to have a higher than expected liquid-phase fraction than the expected fraction calculated using the Henry's law constant (Grosjean and Wright, 1983; van Pinxteren et al., 2005). The relatively long lifespan of MEK (~5 days against for the reaction with OH; Grant et al., 2008) and the high solubility of this oxygenated species (Sander, 2015) suggest that the in situ formation of MEK in

aqueous-phase formation could represent an important source of atmospheric MEK (Rodigast et al., 2016).

As a possible example of this aqueous chemistry source mechanism, we saw a relationship between atmospheric water content (absolute humidity) and MEK emerge during certain periods of summer 2015, specifically around the summer MEK maximum (Figure 13). MEK reached a summer high of 2.47 ppbv at 3:03am on August 8 and therefore at a time when there was no photochemical activity. As MEK began to increase during the early morning of August 8, we also found a significant increase in absolute humidity, which reached a summer maximum of 27.27 kg/m^3 at 6:36am on August 8, three and half hours after MEK peaked. While the peaks are offset, MEK peaked when the absolute humidity was measured at 10.84 kg/m^3 (at 3:03am), more than three times greater than the morning average for summer 2015 (00:00-10:00am mean = 3.13 kg/m^3). The oxygenated nature of MEK opens the potential for partitioning to and from aqueous surfaces (Rodigast et al., 2016).

A third possible explanation could be the high solubility combined with the relatively long lifespan of atmospheric MEK allows for long-range transport from areas with higher mixing ratios of primary VOCs or precursors, such as the Los Angeles Basin or even East Asia (Cooper et al., 2010). We observed high mean and maximum mixing ratios of MEK with long-range westerly flow (Cluster 4) possibly originating over southern California (Table 4, Figure 11). A highly soluble, long-lived species, such as MEK, could be transported by strong flow aloft from the SW to the NFRMA region (Yañez-Serrano et al., 2016; Cooper et al., 2010). Grosjean & Swanson (1983) found elevated levels of MEK in the Los Angeles Basin (up to 15.4 ppbv). There is limited

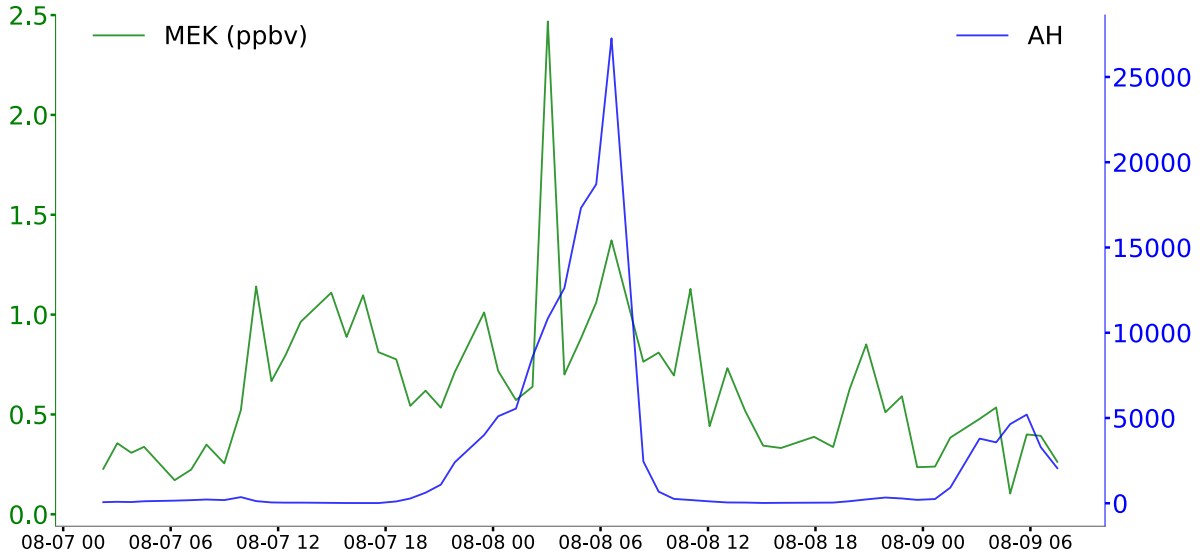

Figure 13. This plot compares absolute humidity (g /m^3) and mixing ratio of MEK (ppbv) for the maximum summer MEK value.

literature on MEK mixing ratios from this area but mixing ratios of other OVOCs (e.g. acetone, acetaldehyde, etc.) have decreased since the 1980s even though they still remain elevated compared to BAO (Warneke et al., 2012). The mean summer mixingratio of acetone in LA (~10ppbv) was almost triple the mean summer mixing ratio from BAO (3.46 ppbv). Additionally, the acetone/CO enhancement ratios have increased by up to 60% from 2002-2010 even as VOC mixing ratios have decreased at an average annual rate of 7.5% (Warneke et al., 2012). Carbon monoxide is commonly used as a tracer of incomplete combustion (and therefore urban and industrial emissions) and has a lifetime of on the order of weeks. This makes CO a good indicator of not only urban and industrial emissions but also can indicate long-range transport. While mixing ratios of OVOCs are lower than previously measured in the source areas

of these trajectories, we believe it is possible that transport from these areas could results in higher mixing ratios of MEK in the NFRMA.

Lastly, direct emissions are also a potential source of MEK since it is used as an industrial solvent and oxidizing agent. There are several locations along the NFRMA that have concentrated industrial activity (Figure 1). For example, Commerce City, CO is an industrial site located north of downtown Denver that has two crude oil refineries that produce motor gasoline, and asphalt (Abeleira, 2017). Commerce City is in the close vicinity to BAO and could be a direct emission source of MEK (~30km to the SSW).

5. CONCLUSIONS

We find strong evidence to suggest that the photo-oxidation of n-butane was an important source of MEK during the daytime hours at BAO in summer 2015. These emissions of n-butane were likely emitted directly from the nearby WGF, one of the largest natural gas fields in the country. While we were able to explain the portion of MEK that was well understood by the PMF solution, there is still a large portion of MEK mixing ratios (>45% by mass and variance) that are unexplained. Possible source factors that warrant future study include long-range transport of primary VOCs and precursors, aqueous chemistry, and direct emission. Understanding how these sources contribute to MEK in the NFRMA will be essential for constraining the regional OH reactivity and radical budget. Future work will apply the analysis developed for the summer data to the spring dataset.

6. ACKNOWLEDGEMENTS

I would like to thank Lynne Gratz and Emily Fischer for all of their work helping me turn this research into something presentable. Thank you to the Fischer and Pierce groups for all their support over the summer while I learned about the dataset and battled with Python. I'd like to thank all who worked to collect and analyze the data from the 2015 field campaign including Jakob Lindaas, Ilana Pollack, Andrew Abeleira, Steven Brey, and the other members of the Chemistry and Atmospheric Science Departments, specifically the Fischer and Farmer groups. I would also like to thank Melissa Burt, the CSU Climate Science REU program and the Dean's Summer Research Grant for providing us the opportunity to conduct this research during summer 2017. Finally, I would like to thank family and friends for their support during all the twists and turns of life.

This work was supported by NOAA under grant number NA14OAR4310148.

REFERENCES

Abeleira, A. et al. (2017), Source characterization of volatile organic compounds in the Colorado Northern Front Range Metropolitan Area during spring and summer 2015, J. Geophys. Res. Atmos., 122, 3595–3613, doi:10.1002/2016JD026227.

Adgate, J., B. Goldstein, and L. McKenzie (2014), Potential Public Health Hazards, Exposures and Health Effects from Unconventional Natural Gas Development, Environ. Sci. Technol., 2014, 48, 8307-8320

Andreae, M. O., and P. Merlet (2001), Emission of trace gases and aerosols from biomass burning, Global Biogeochem. Cycles, 15(4), 955–966, doi:10.1029/2000GB001382.

A.G. Bunch, C.S. Perry, L. Abraham, D.S. Wikoff, J.A. Tachovsky, J.G. Hixon, J.D. Urban, M.A. Harris, L.C. Haws, (2014), Evaluation of impact of shale gas operations in the Barnett Shale region on volatile organic compounds in air and potential human health risks,Science of The Total Environment, 468–469, 832-842, 0048-9697, doi: 10.1016/j.scitotenv.2013.08.080.

Colorado Air Quality Control Commission (2008), Denver Metro Area and North Front Range Ozone Action Plan, Colorado Air Quality Control Commission, Denver, Colo.

Allison, W. (2015), State of Colorado comments, Docket ID EPA-HQ-OAR-2008-0699; FRL-9918-43-OAR.

Atkinson, R., and J. Arey (2003), Atmospheric degradation of volatile organic compounds, Chem. Rev., 103(12), 4605–4638.

Baker, A. K. et al. (2008), Measurements of nonmethane hydrocarbons in 28 United States cities, Atmos. Environ., 42(1), 170–182.

Bon, D. M., et al. (2011), Measurements of volatile organic compounds at a suburban ground site (T1) in Mexico City during the MILAGRO 2006 campaign: Measurement comparison, emission ratios, and source attribution, Atmos. Chem. Phys., 11(6), 2399–2421, doi:10.5194/ acp-11-2399-2011.

Brito, J., et al. (2015)., Vehicular Emission Ratios of VOCs in a Megacity Impacted by Extensive Ethanol Use: Results of Ambient Measurements in São Paulo, Brazil, *Environ. Sci. & Technol. 49* (19), 11381-11387DOI: 10.1021/acs.est.5b03281

Colborn, T., C. Kwiatkowski, K. Schultz, and M. Bachran (2011), Natural gas operations from a public health perspective, Human Ecol. Risk Assess.: An Int. J., 17(5), 1039–1056, doi:10.1080/10807039.2011.605662.

Cooper, O. R., et al. (2010), Increasing springtime ozone mixing ratios in the free troposphere over Western North America, Nature, 463(1), doi: 10.1038/nature08708

Draxler, R. R., and G. D. Hess, 1998: An overview of the HYSPLIT_4 modeling system for trajectories, dispersion, and deposition. *Aust. Meteor. Mag.*, **47**, 295–308.

Energy Information Administration (2013), Natural Gas Annual 2014, U.S. Dept. of Energy Washington, D. C.

de Gouw, J. A., et al., (1999), Emissions of volatile organic compounds from cut grass and clover are enhanced during drying process, Geophys. Res. Lett., 26 (7), 811-814, doi: 10.1029/1999GL900076

de Gouw, J. A., et al., (2003), Sensitivity and specificity of atmospheric trace gas detection by proton-transfer-reaction mass spectrometry, International Journal of Mass Spectrometry, Vol 223-224, 365-382, doi: 10.1016/S1387-3806(02)00926-0

de Gouw, J. A., et al. (2005), Budget of organic carbon in a polluted atmosphere: Results from the New England air quality study in 2002, J. Geophys. Res., 110, D16305, doi:10.1029/2004JD005623.

Goldan, P. D., W. C. Kuster, E. Williams, P. C. Murphy, F. C. Fehsenfeld, and J. Meagher (2004), Nonmethane hydrocarbon and oxy hydrocarbon measurements during the 2002 New England Air Quality Study, *J. Geophys. Res.*, 109, D21309, doi:10.1029/2003JD004455.

Gray, C. M., et al., (2010), Emissions of volatile organic compounds during the decomposition of

plant litter, J. Geophys. Res., 115, G03015, doi:10.1029/2010JG001291.

Grosjean, D., et al., (1983), Carbonyls in Los Angeles air: Contribution of direct emissions and photochemistry, Science of The Total Environment, 29 (1–2), 65-85, 0048-9697, doi: 10.1016/0048-9697(83)90034-7.

Grosjean, D., and Wright, B., (1983), Carbonyls in urban fog, ice fog, cloudwater, and rainwater, Atmospheric Environment, 17 (10), 2093-2096, 0004-6981, doi:10.1016/0004-6981(83)90368-2

Halliday, H. S., et al., (2016), Atmospheric benzene observations from oil and gas production in the Denver-Julesburg Basin in July and August 2014, J. Geophys. Res. Atmos., 121, 11,055–11,074, doi:10.1002/ 2016JD025327.

Jordan, C., et al., (2008), Long-term study of VOCs measured with PTR-MS at a rural site in New Hampshire with urban influences, Atmos. Chem. Phys., 9, 4677-4697, https://doi.org/10.5194/acp-9-4677-2009, 2009.

Katzenstein, A. S., L. A. Doezema, I. J. Simpson, D. R. Blake, and F. S. Rowland (2003), Extensive regional atmospheric hydrocarbon pollution in the southwestern United States, Proc. Natl. Acad. Sci. U.S.A., 100(21), 11,975–11,979, doi:10.1073/pnas.1635258100.

Kirstine, W., I. Galbally, Y. Ye, and M. Hooper (1998), Emissions of volatile organic compounds (primarily oxygenated species) from pasture, J. Geophys. Res., 103(D9), 10605–10619, doi:10.1029/97JD03753.

Lindaas, J., et al. (2017), Changes in ozone and precursors during two aged wildfire smoke events in the Colorado Front Range in summer 2015, Atmos. Chem. Phys., 17, 10691-10707, https://doi.org/10.5194/acp-17-10691-2017

Lindaas, J., (2018), Investigating contributions to elevated surface ozone in the Colorado Front Range during summer 2015, Degree of Master of Science, Colorado State University, Fort Collins, CO.

Liu, Y., Yuan, B., Li, X., Shao, M., Lu, S., Li, Y., Chang, C.-C., Wang, Z., Hu, W., Huang, X., He, L., Zeng, L., Hu, M., and Zhu, T.: Impact of pollution controls in Beijing on atmospheric oxygenated volatile organic compounds (OVOCs) during the 2008 Olympic Games: observation and modeling implications, Atmos. Chem. Phys., 15, 3045-3062, https://doi.org/10.5194/acp-15-3045-2015, 2015.

McKenzie, L. M., R. Z. Witter, L. S. Newman, and J. L. Adgate (2012), Human health risk assessment of air emissions from development of unconventional natural gas resources, Sci. Total Environ., 424, 79–87, doi:10.1016/j.scitotenv.2012.02.018.

Mellouki, A., Wallington, T. J., and Chen, J. (2015), Atmospheric Chemistry of Oxygenated Volatile Organic Compounds: Impacts on Air Quality and Climate (2015)
Chemical Reviews, *115* (10), 3984-4014, doi: 10.1021/cr500549n

Müller, K., et al., (2006), Biogenic carbonyl compounds within and above a coniferous forest in Germany, Atmospheric Environment, 40 (1), 81-91, 1352-2310, doi: 10.1016/j.atmosenv.2005.10.070.

Parsons, Z., and Arnold, S., (2004) Ozone Transport in the West: An Exploratory Study, Western States Air Resources Council, Colorado Department of Public Health and Environment

Pétron, G., et al. (2012), Hydrocarbon emissions characterization in the Colorado Front Range: A pilot study, J. Geophys. Res., 117, D04304, doi:10.1029/2011JD016360.

Rodigast, M., Mutzel, A., Schindelka, J., and Herrmann, H.: A new source of methylglyoxal in the aqueous phase, Atmos. Chem. Phys., 16, 2689-2702, https://doi.org/10.5194/acp-16-2689-2016, 2016.

Singh, H. B., and P. L. Hanst (1981), Peroxyacetyl nitrate (PAN) in the unpolluted atmosphere: An important reservoir for nitrogen oxides, Geophys. Res. Lett., 8(8), 941–944, doi:10.1029/GL008i008p00941

Singh, H. B., (1987), Reactive nitrogen in the troposphere, *Environmental Science & Technology*, *21* (4), 320-327, DOI: 10.1021/es00158a001

Singh, H. B., et al., (1995), High concentrations and photochemical fate of oxygenated hydrocarbons in the global troposphere, Nature, 378, 50, doi: 10.1038/378050a0

Singh, H., et al. (2004), Analysis of the atmospheric distribution, sources, and sinks of oxygenated volatile organic chemicals based on measurements over the Pacific during TRACE-P, J. Geophys. Res., 109, D15S07, doi:10.1029/2003JD003883

Sommariva, R., et al. (2008), A study of organic nitrates formation in an urban plume using a master chemical mechanism, Atmos. Environ., 42(23), 5771–5786.

Song, G. C., & Ryu, C.-M. (2013). Two Volatile Organic Compounds Trigger Plant Self-Defense against a Bacterial Pathogen and a Sucking Insect in Cucumber under Open Field Conditions. *International Journal of Molecular Sciences*, *14*(5), 9803–9819. http://doi.org/10.3390/ijms14059803

Swarthout, R. F., R. S. Russo, Y. Zhou, A. H. Hart, and B. C. Sive (2013), Volatile organic compound distributions during the NACHTT campaign at the Boulder Atmospheric Observatory: Influence of urban and natural gas sources, J. Geophys. Res. Atmos., 118, 10,614–10,637, doi:10.1002/jgrd.50722.

Swarthout, R. F., et al (2015), Impact of Marcellus Shale Natural Gas Development in Southwest Pennsylvania on Volatile Organic Compound Emissions and Regional Air Quality, *Environmental Science & Technology*, *49* (5), 3175-3184, DOI: 10.1021/es504315f

Thompson, C. R., J. Hueber, and D. Helmig (2014), Influence of oil and gas emissions on ambient atmospheric non-methane hydrocarbons in residential areas of Northeastern Colorado, Elementa Sci. Anthropocene, 2, 000035, doi:10.12952/journal.elementa.000035.

Warneke, C., J. A. de Gouw, J. S. Holloway, J. Peischl, T. B. Ryerson, E. Atlas, D. Blake, M. Trainer, and D. D. Parrish (2012), Multiyear trends in volatile organic compounds in Los Angeles, California: Five decades of decreasing emissions, J. Geophys. Res., 117, D00V17, doi:10.1029/2012JD017899.

Wheatley, R., (1997), Effect of substrate composition on production of volatile organic compounds from Trichoderma spp. Inhibitory to wood decay fungi,, International Biodeterioration & Biodegradation, 39(2–3), 199-205, 0964-8305, doi: 10.1016/S0964-8305(97)00015-2

Yáñez-Serrano, A. M., Nölscher, A. C., Bourtsoukidis, E., Derstroff, B., Zannoni, N., Gros, V., Lanza, M., Brito, J., Noe, S. M., House, E., Hewitt, C. N., Langford, B., Nemitz, E., Behrendt, T., Williams, J., Artaxo, P., Andreae, M. O., and Kesselmeier, J.: Atmospheric mixing ratios of methyl ethyl ketone (2-butanone) in tropical, boreal, temperate and marine environments, Atmos. Chem. Phys., 16, 10965-10984, https://doi.org/10.5194/acp-16-10965-2016, 2016